Fifth International Conference on Sustainable Construction Materials and Technologies. http://www.claisse.info/Proceedings.htm

PREPARATION FOR GREEN HIGH PERFORMANCE STEAM-CURED CONCRETE

Youjun Xie, Lou Chen, Keren Zheng, Guangcheng Long, Cong Ma, Jin Zhou, Ye Shi
Civil Engineering School, Central South University, 68 Shaoshan South Road,
Changsha City, Hunan Province, China,
Email：longguangcheng@csu.edu.cn；xieyj@csu.edu.cn; zhengkeren@csu.edu.cn

ABSTRACT

In China, steam-cured concrete precast elements are increasingly applied in prefabricated buildings and rail transit systems such as high-speed railways. However, traditional steam curing technology not only consumes lots of energy but also brings about problems such as surface cracks, embrittlement, and deteriorative long-term performance. This paper reports an investigation on preparing high performance steam-cured concrete by optimizing the compositions of cementitious materials and reducing the stream curing temperature. Furthermore, the associated reduction in CO_2 emissions and energy consumption were estimated. Whit the incorporation of metakaolin of very high reactivity, the concrete stream-cured at 40^{o}C reached satisfactory early-age strength and exhibits low permeability and lowered carbon footprint. The CO_2 emission was reduced by 20% in comparison with the conventional steam curing technology.

Keywords: Steam-cured concrete; Binder system composition; Carbon dioxide emission

1. INTRODUCTION

Steam curing, which accelerates early strength development of concrete by means of elevating temperature and providing moisture simultaneously, is commonly used in the production of precast concrete products and elements for high productivity (ACI-517, 1992).

However, steam curing brings about problems such as weakened surface quality, coarsened microstructure, recession in strength at later ages, and other deteriorative long-term performance (ACI-305, 1991; Escalante-Garcıa and Sharp, 2001; He, 2012; Kim et al., 2002), which influence the integrity of elements and structure durability.

Partially replacing cement with supplementary cementitious materials (SCMs) in steam-cured concrete is helpful to mitigate the above-mentioned adverse effects as well as reduce the CO_2 footprint (Ho et al., 2003; Liu et al., 2005). For instance, Liu (Liu et al., 2005) reported that the incorporation of ground granulated blast furnace slag (GGBS) and ultrafine fly ash (UFA) leads to an improved compressive strength gain of steam-cured concrete at late ages. Ho (Ho et al., 2003) found that steam-cured concrete incorporated with silica fume (SF) exhibits higher compressive strength and lower

sorptivity in comparison to that with Ordinary Portland cement(OPC) exclusively. Nevertheless, the use of SCMs can only mitigate the adverse effects to some extent, steam-cured concrete incorporated with SCMs still suffers from the heat-induced problems (He, 2012). In order to improve the homogeneity of microstructure, decrease the thermal gradient, mitigate heat damage effect, and reduce energy consumption, lowering the maximum curing temperature seems to be an efficient way. However, lowering the maximum curing temperature would hinder early strength development, which is of great importance in the precast industry. The use of SCMs with high reactivity in steam-cured concrete may be a promising way to reduce the maximum curing temperature without compromising early strength gain.

Recently, there are increasing research interests in using metakaolin for its excellent pozzolanic properties (Fernandez et al., 2011; Souza and Dal Molin, 2005). Investigations showed that the substitution of 10%-25% cement (by mass) by metakaolin results in an increased or comparable 1-day and 28-day compressive strength in contrast to concrete or mortar incorporating cement only (Cassagnabère et al., 2009; Cassagnabère et al., 2010; Shen et al., 2017). The corresponding microstructure tests demonstrated that the incorporation of metakaolin enables to consume $Ca(OH)_2$ at early stages, and the formation of secondary C-A-S-H refines the pore structure, leading to an improved early mechanical property. Besides, the addition of MK contributes to an enhanced volume stability for normal-cured concrete, and further decreases the autogenous and drying shrinkage to some extent as well (Brooks and Megat Johari, 2001; Gleize et al., 2007; Güneyisi et al., 2008; Ismail and Hassan, 2016).

Compared to MK, the less reactive limestone powder (LS) is more used as inert filler. Nevertheless, within limits, the calcite in limestone can interact with aluminum-bearing phases or metakaolin to form mono/hemi-carboaluminate phases which exhibit better thermodynamic stability than ettringite or monosulphoaluminate(Matschei, T. et al., 2007a; Matschei, Thomas et al., 2007b). Furthermore, a strongly synergistic effect between limestone powder and metakaolin has been recently reported (Antoni et al., 2012; Nied et al., 2015; Puerta-Falla et al., 2015; Sánchez Berriel et al., 2016; Tironi et al., 2015; Vance et al., 2013). The reaction between calcite from limestone powder and aluminum-bearing phases promotes both reactions of MK and OPC, producing supplementary aluminate phases, leading to an increased solid phase volume and a refined microstructure at late-age consequently. However, the performance of concrete blended with combination of MK and LS exposed to steam curing is still largely unknown.

This research focuses on the preparation of green high performance steam-cured concrete by optimizing binder system and curing regime. Based on the above premises, therefore, this study aims to utilize the high reactivity of MK and its synergistic effect with limestone powder to achieve a satisfactory early-age mechanical property and to improve the long-term performance at a lowered steam curing temperature so that the heat-induced adverse effect would be mitigated. Investigations on mechanical property, sorptivity, and the carbon dioxide emission of concrete incorporated with the combination of MK and limestone powder, which were subjected to a regular steam-

curing cycle with a maximum curing temperature of 60 ºC and one with a maximum curing temperature of 40 ºC respectively were carried. A typical steam-cured concrete incorporated with GGBS and FA is set as a reference for comparison purpose, which have the same compressive strength as the steam-cured concrete without supplementary cement materials substitution. A life cycle assessment technique was used to estimate the carbon dioxide reduction of the designed steam-cured concrete.

2. EXPERIMENTS

2.1 Materials

Type P.I 42.5 Portland cement (similar to CEM I or ASTM Type III) was used. GGBS, FA (class F), MK, and LS were used as SCMs. The chemical composition and the particle size distribution of used materials are presented in Table 1 and Fig.1, respectively. The coarse and fine aggregates were crushed gravel with size of 5-20 mm and river sand with a fineness modulus of 2.8.

Table 1. Chemical composition of raw materials used [%]

	Cement	MK	LS	GGBS	FA
CaO	61.6	0.4	75.8	53.3	3.8
SiO_2	19.0	51.1	0.3	26.1	46.0
Al_2O_3	4.3	45.3	0.1	11.7	38.0
Fe_2O_3	3.0	0.5	-	-	5.5
SO_3	3.6	0.1	0.1	1.5	0.8
NaO_2	0.1	0.2	-	0.2	0.2
K_2O	0.8	0.2	-	0.3	0.5
MgO	2.2	0.1	0.2	6.0	0.4
TiO_2	0.18	1.1	-	0.7	1.1
Rest	0.1	0.1	0.1	0.1	0.3
LOI	1.2	0.8	44.0	0.9	7.6

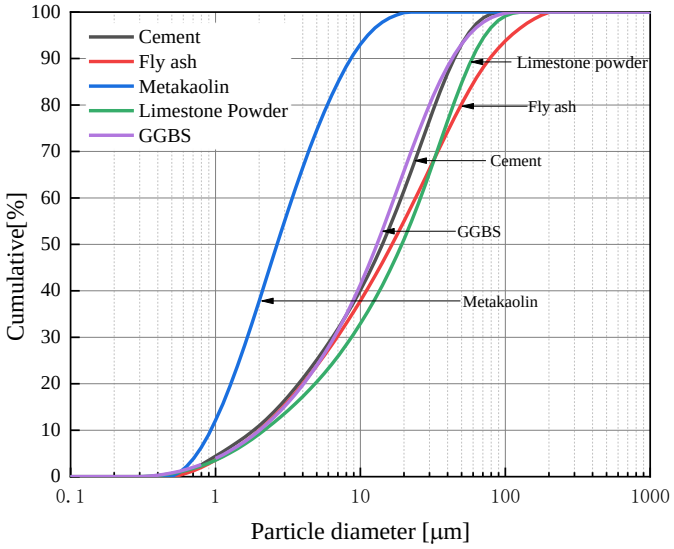

Fig.1 Particle size distribution of raw materials

2.2 Mix Proportions of Concrete and Paste

A commonly used mix proportion for the prefabricated concrete slab, sleeper in China is shown in Table 2. The mix proportion was optimized by substituting cement with 20% of slag and 10% of FA (He, 2012). For compare purpose, GGBS and FA were replaced by MK and LS equivalently as shown in Table 2. Limestone powder was incorporated as filler to reduce the hydration heat, improve the volume stability during steam curing, and to react synergistically with MK at late ages to improve the long-term performance of steam-cured concrete. Superplasticizer was added to obtain appropriate workability.

Table 2. Mix proportions of concrete

	Cement	MK	LS	GGBS	FA	Sand	CG*	Water	SP**
CML	315	90	45	-	-	660	1210	135	4.5
CGF	315	-	-	90	45	660	1210	135	2.25

* Crushed gravel

** SP=Superplasticizer

2.3 Methods

2.3.1 Strength Measurement

Cubic concrete specimens of 100 mm ×100 mm ×100 mm were cast for compressive strength and sorptivity tests. After placement, concrete specimens were subjected to two different steam curing cycles with maximum temperatures of 40 ºC and 60 ºC, and the latter one is a typical steam-curing cycle used in the production of prefabricated elements in China. The two steam curing cycles are schematically shown in Fig. 2. Once cooled down to room temperature (20 ºC), the steam cured concrete specimens were demoulded and transferred to a climate room (20±1 ºC, RH≥ 95%) for further curing. The compressive strength tests of concrete were conducted on 3 specimens of each mix at ages of 1d, 7 d, 28 d, and 90 d.

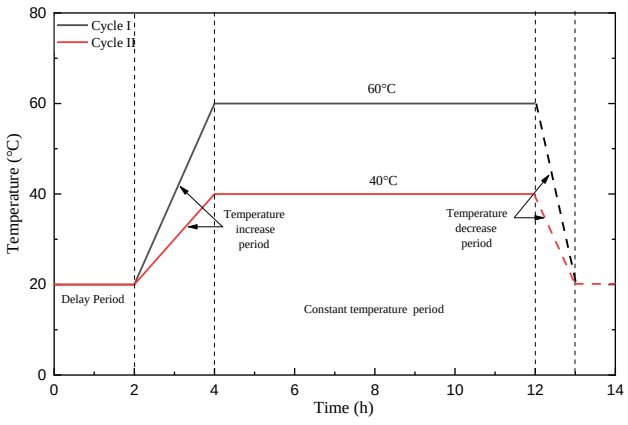

Fig. 2 Schematic of two steam-curing cycles used in the study

2.3.2 Sorptivity Test

For the sorptivity test, 3 steam-cured concrete specimens (100 mm×100 mm×100 mm) of each mix were taken out from the climate room at ages of 1d, 7d, 28 and 90 d, subsequently oven-dried at 60 ºC to constant weight, then sealed with paraffin on the end and two opposite sides. After that, the finishing surface was immersed into water at depth of 5 mm and the water level was kept the same during the whole test. At each time interval, specimens were taken out from the water container, mopped off the excess surface water with a damp tissue, and weighed on a digital balance. The whole process was completed in 30 s according to (Hall, 1989). To calculate the sorption coefficient, obtained data were fitted to equation

$$i = St^{1/2} + S_0 \quad (1)$$

where i is water volume absorbed per unit cross-section area, S is the sorptivity coefficient, t is the time and S_0 is a correction term added to account for surface effects at the time sample is placed in contact with water.

3. RESULTS AND DISCUSSION

3.1 Strength

Compressive strength of concrete steam-cured at 40 ºC and 60 ºC are given in Fig.3 (a) and specific compressive strength normalized to the reference (CGF-60ºC, steam-cured at 60 ºC) are presented in Fig.3 (b). As can be seen, although the decrease in the maximum curing temperature led to a reduced compressive strength at 1 day, concrete steam-cured at 40 ºC gained higher strength at late ages in comparison with concrete steam-cured at 60 ºC. This is attributed to the adverse effect of temperature on compressive strength from 7 d onwards, which has been disclosed by many published literature (Kim et al., 2002; Paul, 1958; Verbeck, 1968).

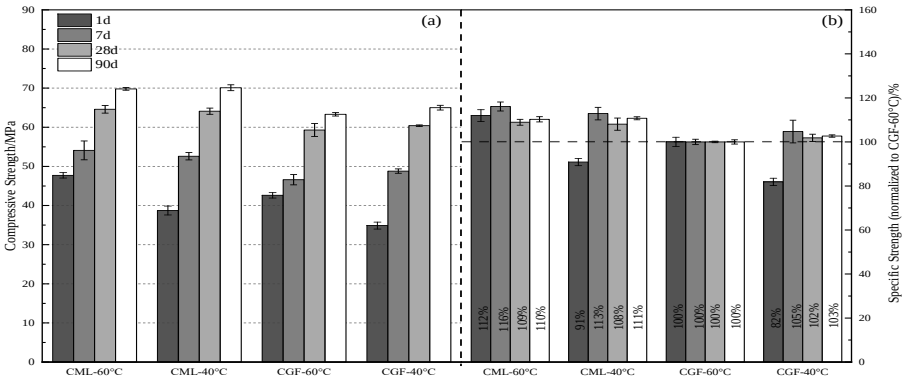

Fig.3 Compressive strength of steam-cured concrete (a) and specific strength normalized to CGF-60ºC (b) from 1d to 90d

Due to the excellent reactivity of metakaolin, CML specimens exhibited higher compressive strength than that of CGF specimens at all ages when steam cured at the same temperatures. Furthermore, CML specimens cured at 40 ºC gained comparable 1 d strength with respect to CGF specimens steam cured at 60 ºC. The compressive

strength of CML specimens steam cured at 40 ºC (CML-40ºC) can reach ~ 91% of that of CGF-60 ºC (Fig.4 (b)). This is of great significance for the decrease in curing temperature can not only mitigate the adverse effect arising from elevated temperatures on long-term performance, but also help to save energy for steam curing notably.

3.2 Sorptivity

Sorptivity is commonly used as a parameter to assess the surface quality and durability of concrete as it characterizes the capability to absorb and transmit water in non-saturated state (Ho et al., 2003). Fig.4 shows the results of water sorption tests based on measurements of gained weight and sorptivity coefficient at 1 d, 7 d, 28 d, and 90 d. It is obvious that the weight of water absorbed (WA) gradually increased within 24 h while the uptake rate of water decreased as indicated by the decreased slope of curves. Generally, the whole process of sorptivity test can be divided into two linear stages. In the first stage with a higher slope, sorptivity coefficient is related to the capillary suction; and the lower one in the second stage is attributed to the filling of pores and air voids (Martys and Ferraris, 1997).

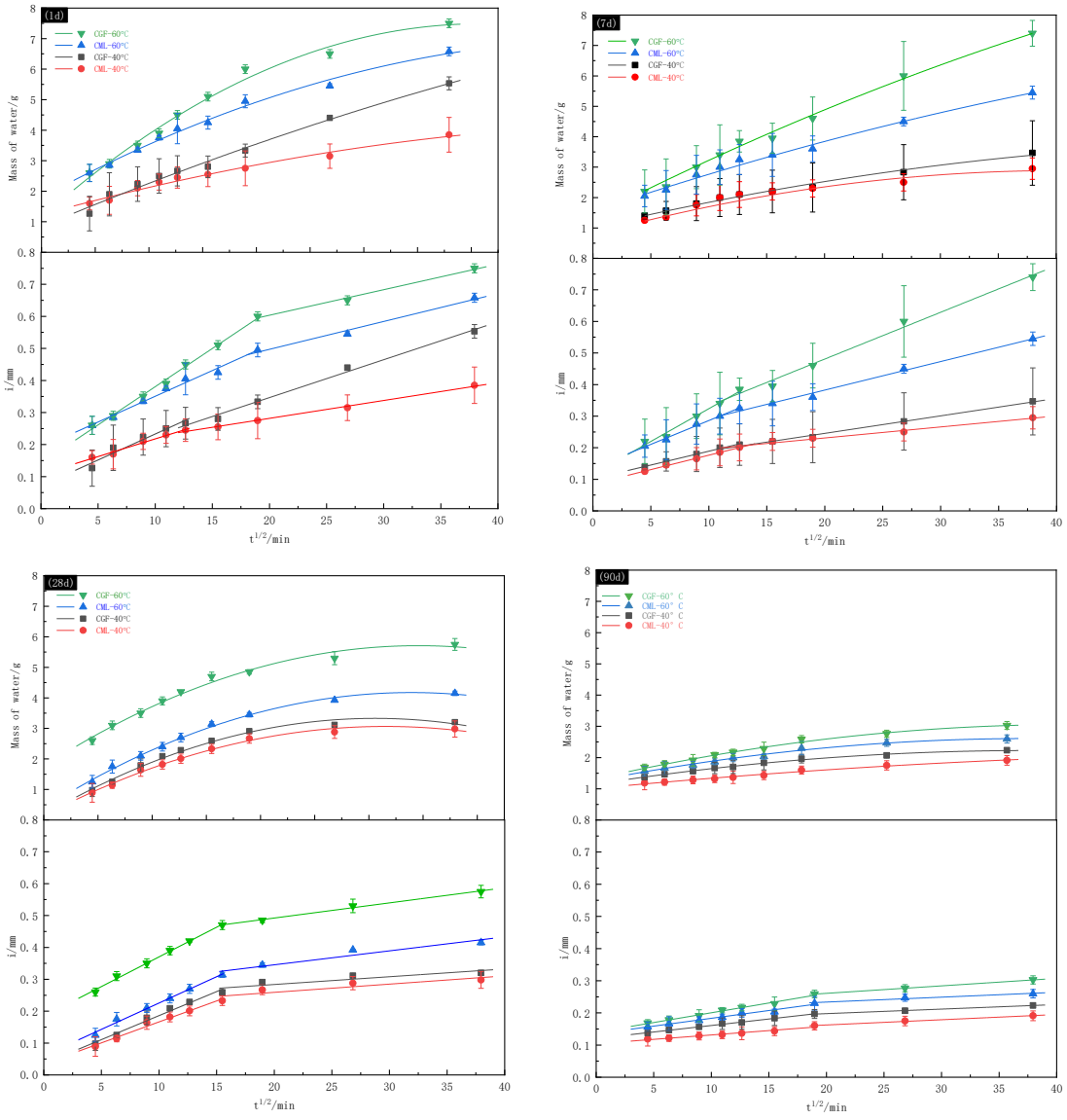

Fig.4 Water sorptivity and sorptivity coefficient of stream-cured concrete at 1d, 7d, 28d, and 90d

As can be seen, the WA value and sorptivity coefficient for specimens cured at 60 ºC (CGF-60 ºC, CML-60 ºC) were significantly higher than those cured at 40ºC (CGF-40 ºC, CML-40 ºC). These results are in accordance with earlier findings (Cano Barrita et al., 2003; Ho et al., 2003), suggesting that the higher curing temperature contributes to a more open pore structure in the near-surface of concrete specimens.

Subjected to steam curing cycle with the same maximum temperature, concrete specimens incorporated with MK and limestone powder showed lower WA values. It should be noted that the WA value of CML-60 is much lower than that of CGF-60 ºC and close to the value of CGF-40 ºC and CML-40 ºC. In addition, the WA values of each specimen decreased from the age of 1d to 90 d, and this can be explained by considering the continuous hydration process which generates hydration products to refine the pore structure.

Generally, a linear relationship between the compressive strength and WA value was observed, except for several values at 90d as shown in Fig.5. It is clearly illustrated that higher steam curing temperature resulted in a higher WA value within the similar compressive strength level. This phenomenon also has been verified by several published literature (Cano Barrita et al., 2003; Long et al., 2012), the possible explanations are: (i) the higher temperature accelerates the hydration process, leading to a more coarsened microstructure; (ii) severer moisture transfer and loss take place at the near-surface area, especially during the cooling stage and thereby forming a more open pore structure; (iii) a larger temperature gradient is inclined to appear at higher curing temperature which may lead to surface cracks. When subjected to the same steam-curing cycles, CML specimens exhibited lower WA value in comparison with CGF specimens. It can thus be implicated that the CML specimens have a better near-surface quality.

3.3 The Carbon Dioxide Emission of the Steam-Cured Concrete

The e-CO_2 of concrete generated in the major processes including raw materials processing, transportation, production, and curing phases of the concrete is calculated (Yang et al. 2013). But the CO_2 emission of concrete produced during transportation and production is not considered in this investigation owing to its small contribution on environmental burden (Long et al., 2015). Therefore, the total CO_2 emissions of steam-cured concrete are calculated by summing the e-CO_2 in the raw material and curing phase.

The e-CO_2 in the raw materials can be acquired by summing up the products of e-CO_2 of each raw material and the unit volume weight of materials. The embodied carbon dioxide of the raw materials is presented in Table 3. Therefore, the CO_2 emission of the steam-cured concrete incorporated with the combination of metakaolin and limestone is 310.6 kg/m^3. The carbon dioxide emission of the steam-cured concrete without supplementary cement materials substitution is about 382.6 kg/m^3.

Table 3. Embodied carbon dioxide (e-CO_2) of the raw materials of concrete

Items	Embodied-CO_2	References

Cement	0.83	Long et al., 2015
Fly ash	0.009	Long et al., 2015
GGBS	0.019	Long et al., 2015
Metakaolin	0.4	Long et al., 2015
Limestone	0.017	Müller et al., 2014
Sand	0.001	Müller et al., 2014
Superplasticizer	0.72	Long et al, 2015
Crushed gravel	0.007	Müller et al., 2014

The saved energy due to the lowered maximum curing temperature was calculated roughly based on the algorithms established by Won et al. (Won et al., 2013). The specific heat of the concrete is 1170 J/kg ^{o}C·(Neville, 2011) and the hydration heat for type I cement at 40 ^{o}C and 60 ^{o}C for 14 hours are 184 kJ/kg and 218 kJ/kg respectively (Association, 1997; Ma et al., 1994). The heat loss is related to the heat conductivity of curing cover, the temperature gradient between inside and outside can be calculated by Eq. (4). The reciprocal of heat transmitter rate U is determined by heat transfer coefficient of the inner and outer surface, the thickness of curing cover and heat conductivity. (Bergman et al., 2011).The specific heat of concrete, heat conductivity of curing cover, cover thickness, heat transfer coefficient of the inner side and outer side, and boiler efficiency adopted in the calculation were given in Table. 4 in the appendix. The whole calculative process was present in Eq.(2) to Eq.(5) in the appendix. The saved energy for 1m^3 steam concrete based on the conservative calculation is around 73.4%, reducing CO_2 emission by 18.84 kg.

Therefore, the carbon dioxide emission of CML-40 ^{o}C is 317.4 kg/m^3. The CO_2 emission of the steam-cured reference concrete under 60 ^{o}C curing is about 408.3 kg/m^3. This indicated that the carbon dioxide emission of steam-cured concrete incorporated with the combination of metakaolin and limestone when curing at 40 ℃ isothermal temperature was about 23% lower than that of the control mix without supplementary cement materials substitution and 60 ℃ of steam curing.

4. CONCLUSION

(1) The reduction in the maximum curing temperature improves sorptivity and long-term mechanical property of steam-cured concrete significantly, although higher steam-curing temperatures lead to higher early-age strength.

(2) Due to its excellent pozzolanic reactivity, the incorporation of metakaolin promotes early strength gain for steam-cured concrete, thus enabling to reduce the maximum curing temperature without compromising early strength. The synergistic effect between limestone powder and metakaolin promotes both reactions of metakaolin and Portland cement, hence reducing long-term sorptivity and improving mechanical properties of steam-cured concrete.

(3) The study also reveals the feasibility of reducing steam curing temperatures by using metakaolin of high reactivity, which is of significance for mitigating steam-curing induced detrimental effects and reducing carbon dioxide emission.

Acknowledgment

The study was supported by National Natural Science Foundation of China (NSFC) [grant number U1534207 & 51578551].

APPENDIX

Abbreviations Used in Calculations

Q_t-total heat energy

Q_{tr}-heat needed for temperature rising stage

Q_{hd}-heat dissipation from the initial of temperature rising stage until the end of maximum temperature curing stage

Q_{hc}-hydration heat of cement

C_c - specific heat of concrete

m – mass of steam cured concrete

K_c – heat conductivity of curing cover

h_{in} – convection heat transfer coefficient of inner side (saturated steam)

h_{out} – convection heat transfer coefficient of outer side (air at 20°C, 40%RH)

U-heat transmittance rate J/m^2·s· °C

A-area exposed to outside

T_{in}- inside temperature

T_{out}-outside temperature

t1-start time of temperature rising stage

t2-end time of temperature rising stage

t3-end time of maximum temperature curing stage

$$Q_t = (Q_{tr} + Q_{hd})/\alpha \quad (2)$$

$$Q_{tr} = C_c \times m \times (T_{max} - T_{pre}) - Q_h \quad (3)$$

$$Q_{hd} = \int_{t1}^{t2} U \times A \times (T_{in} - T_{out})\, dt + U \times A \times (T_{in} - T_{out}) \times (t3 - t2) \quad (4)$$

$$\frac{1}{U} = \frac{1}{h_{out}} + \frac{T}{K_c} + \frac{1}{h_{in}} \quad (5)$$

Table 4. Parameters for energy consumption calculation

Classification	Value	Reference
Specific heat of concrete （J/ kg· °C）	1170	(Neville, 2011)
Heat conductivity of curing cover （kJ/m·h·K）	670	(Won et al., 2013)
Thickness of curing cover (m)	0.02	
Heat transfer coefficient of saturated steam (inner side) （kJ/m^2·h·K）	108	(Bergman et al., 2011)
Heat transfer coefficient of air at 20 °C (40% RH) (outside) （kJ/m^2·h·K）	18	(Bergman et al., 2011)
Efficiency of boiler	0.8	

REFERENCE:

ACI-305, 1991. Hot weather concreting. ACI Material J 88, 417-436.

ACI-517, 1992. Accelerated Curing of Concrete at Atmospheric Pressure -State of the Art. Journal Proceedings 77(6).

Antoni, M., Rossen, J., Martirena, F., Scrivener, K., 2012. Cement substitution by a combination of metakaolin and limestone. Cement and Concrete Research 42(12), 1579-1589.

Association, P.C., 1997. Portland cement, concrete, and heat of hydration. Concrete Technology Today 18(2), 1-4.

Bergman, T.L., Incropera, F.P., DeWitt, D.P., Lavine, A.S., 2011. Fundamentals of heat and mass transfer. John Wiley & Sons.

Brooks, J.J., Megat Johari, M.A., 2001. Effect of metakaolin on creep and shrinkage of concrete. Cement and Concrete Composites 23(6), 495-502.

Cano Barrita, F.d.J., Bremner, T., Balcom, B., 2003. Effects of curing temperature on moisture distribution, drying and water absorption in self-compacting concrete. Magazine of Concrete Research 55(6), 517-524.

Cassagnabère, F., Escadeillas, G., Mouret, M., 2009. Study of the reactivity of cement/metakaolin binders at early age for specific use in steam cured precast concrete. Construction and Building Materials 23(2), 775-784.

Cassagnabère, F., Mouret, M., Escadeillas, G., Broilliard, P., Bertrand, A., 2010. Metakaolin, a solution for the precast industry to limit the clinker content in concrete: Mechanical aspects. Construction and Building Materials 24(7), 1109-1118.

Escalante-Garcıa, J., Sharp, J., 2001. The microstructure and mechanical properties of blended cements hydrated at various temperatures. Cement and Concrete Research 31(5), 695-702.

Fernandez, R., Martirena, F., Scrivener, K.L., 2011. The origin of the pozzolanic activity of calcined clay minerals: A comparison between kaolinite, illite and montmorillonite. Cement and Concrete Research 41(1), 113-122.

Gleize, P.J.P., Cyr, M., Escadeillas, G., 2007. Effects of metakaolin on autogenous shrinkage of cement pastes. Cement and Concrete Composites 29(2), 80-87.

Güneyisi, E., Gesoğlu, M., Mermerdaş, K., 2008. Improving strength, drying shrinkage, and pore structure of concrete using metakaolin. Materials and Structures 41(5), 937-949.

Hall, C., 1989. Water sorptivity of mortars and concretes: a review. Magazine of concrete research 41(147), 51-61.

He, Z., 2012. Heat damage effects of steam curing on concrete and corresponding improvement measures （in Chinese）. Central South University, p. 165.

He, Z., Long, G., Xie, Y., Liu, J., 2014. Surface layer degradation effect of steam cured concrete (in Chinese). Jianzhu Cailiao Xuebao: Journal of Building Materials 17(6).

Ho, D., Chua, C., Tam, C., 2003. Steam-cured concrete incorporating mineral admixtures. Cement and concrete research 33(4), 595-601.

Ismail, M.K., Hassan, A.A.A., 2016. Use of metakaolin on enhancing the mechanical properties of self-consolidating concrete containing high percentages of crumb rubber.

Journal of Cleaner Production 125, 282-295.

Kim, J.-K., Han, S.H., Song, Y.C., 2002. Effect of temperature and aging on the mechanical properties of concrete: Part I. Experimental results. Cement and Concrete Research 32(7), 1087-1094.

Liu, B., Xie, Y., Li, J., 2005. Influence of steam curing on the compressive strength of concrete containing supplementary cementing materials. Cement and Concrete Research 35(5), 994-998.

Long, G., He, Z., Omran, A., 2012. Heat damage of steam curing on the surface layer of concrete. Magazine of Concrete Research 64(11), 995-1004.

Long, G., Gao, Y., & Xie, Y., 2015. Designing more sustainable and greener self-compacting concrete. Construction & Building Materials, 84, 301-306.

Ma, W., Sample, D., Martin, R., Brown, P., 1994. Calorimetric Study of Cement Blends Containing Fly Ash, Silica Fume, and Slag at Elevated Temperatures. Cement, concrete and Aggregates 16 (8), 93-99.

Martys, N.S., Ferraris, C.F., 1997. Capillary transport in mortars and concrete. Cement and Concrete Research 27(5), 747-760.

Matschei, T., Lothenbach, B., Glasser, F.P., 2007a. The role of calcium carbonate in cement hydration. Cement and Concrete Research 37(4), 551-558.

Matschei, T., Lothenbach, B., Glasser, F.P., 2007b. Thermodynamic properties of Portland cement hydrates in the system CaO–Al2O3–SiO2–CaSO4–CaCO3–H2O. Cement and Concrete Research 37(10), 1379-1410.

Müller, H. S., Haist, M., & Vogel, M., 2014. Assessment of the sustainability potential of concrete and concrete structures considering their environmental impact, performance and lifetime. Construction & Building Materials, 67, 321-337.

Neville, A.M., 2011. Properties of concrete.

Nied, D., Stabler, C., Zajac, M., 2015. Assessing the Synergistic Effect of Limestone and Metakaolin, Calcined Clays for Sustainable Concrete. Springer, pp. 245-251.

Paul, K., 1958. Effect of Mixing and Curing Temperature on Concrete Strength. Journal Proceedings 54(6).

Puerta-Falla, G., Balonis, M., Le Saout, G., Neithalath, N., Sant, G., 2015. The Influence of Metakaolin on Limestone Reactivity in Cementitious Materials, Calcined Clays for Sustainable Concrete. Springer, pp. 11-19.

Sánchez Berriel, S., Favier, A., Rosa Domínguez, E., Sánchez Machado, I.R., Heierli, U., Scrivener, K., Martirena Hernández, F., Habert, G., 2016. Assessing the environmental and economic potential of Limestone Calcined Clay Cement in Cuba. Journal of Cleaner Production 124, 361-369.

Shen, P., Lu, L., Chen, W., Wang, F., Hu, S., 2017. Efficiency of metakaolin in steam cured high strength concrete. Construction and Building Materials 152, 357-366.

Souza, P.S.L., Dal Molin, D.C.C., 2005. Viability of using calcined clays, from industrial by-products, as pozzolans of high reactivity. Cement and Concrete Research 35(10), 1993-1998.

Tironi, A., Scian, A.N., Irassar, E.F., 2015. Ternary blended cement with limestone filler and kaolinitic calcined clay, Calcined Clays for Sustainable Concrete. Springer, pp. 195-201.

Vance, K., Aguayo, M., Oey, T., Sant, G., Neithalath, N., 2013. Hydration and strength development in ternary portland cement blends containing limestone and fly ash or metakaolin. Cement and Concrete Composites 39, 93-103.

Won, I., Na, Y., Kim, J.T., Kim, S., 2013. Energy-efficient algorithms of the steam curing for the in situ production of precast concrete members. Energy and Buildings 64, 275-284.

Yang, K. H., Song, J. K., Song, K. I., 2013. Assessment of CO_2, reduction of alkali-activated concrete. Journal of Cleaner Production, 39(1), 265-272.